# Systematic study of effects of growth conditions on the (nano-, meso-, micro)size and (one-, two-, three-dimensional) shape of GaN single crystals grown by a direct reaction of Ga with ammonia

Aya Moustafa Sayed ElAhl, Maoqi He, Peizhen Zhou, G. L. Harris, Lourdes Salamanca-Riba, Frederick Felt, Harry C. Shaw, Ashok Sharma, Muzar Jah, Darryl Lakins, Todd Steiner, and S. Noor Mohammad

Citation: Journal of Applied Physics **94**, 7749 (2003); doi: 10.1063/1.1622992
View online: http://dx.doi.org/10.1063/1.1622992
View Table of Contents: http://scitation.aip.org/content/aip/journal/jap/94/12?ver=pdfcov
Published by the AIP Publishing



# Systematic study of effects of growth conditions on the (nano-, meso-, micro)size and (one-, two-, three-dimensional) shape of GaN single crystals grown by a direct reaction of Ga with ammonia

Aya Moustafa Sayed ElAhl, Maoqi He, Peizhen Zhou, and G. L. Harris
*Materials Science Research Center of Excellence, Howard University, Washington, D.C. 20059*

Lourdes Salamanca-Riba
*Department of Materials & Nuclear Engineering, University of Maryland at College Park, College Park, Maryland 20742*

Frederick Felt, Harry C. Shaw, Ashok Sharma, Muzar Jah, and Darryl Lakins
*Component Technology & Radiation Effects Branch, NASA Goddard Space Flight Center, Greenbelt, Maryland 20771*

Todd Steiner
*Air Force Laboratory, Air Force Office of Scientific Research, 801 North Randolph Street Suite 900, Arlington, Virginia 22203*

S. Noor Mohammad[a)]
*Department of Electrical Engineering and the Materials Science Research Center of Excellence, Howard University, 2300 Sixth Street NW, Washington, D.C. 20059*

(Received 11 April 2003; accepted 10 September 2003)

A series of experiments have been conducted to systematically study the effects of growth conditions ($NH_3$ flow rate, growth temperature, chamber pressure, and growth location) on the size (nano, meso, or micro) and the shape (one, two, or three dimensional) of GaN single crystal products grown by a direct reaction of Ga with $NH_3$. A growth map with a wider range of experimental parameters was developed; it has three distinct zones. The size and shape of the products in every zone were found to depend on both temperature and $NH_3$ flow rate with other growth conditions fixed. An *effective surface diffusion length* consisting of the Ga atomic surface diffusion length and the GaN molecular surface diffusion length, and the *anisotropy* of the Ga surface diffusion length and the GaN growth rate in different growth directions were introduced into the growth model, in such a way that it allowed successful explanation of all observed results. The optimal growth parameters could thus be determined, which conclusively demonstrated that nanowires with uniform diameter, clear crystal structure, length larger than 1 mm, uniform location distribution, and high yield can be obtained. Such a growth map based on in-depth understanding of the growth mechanism provides a clear direction for growing various materials with desired size and shape. © *2003 American Institute of Physics.* [DOI: 10.1063/1.1622992]

## I. INTRODUCTION

Nanowires are very promising as elemental building blocks for nanotechnology applications.[1–5] Among them, GaN nanowires exhibit large energy band gaps and structural confinement, which are useful for realizing nanosize ultraviolet or blue emitters, detectors, high-speed field-effect transistors, and high-temperature microelectronic devices.[6,7] However, these electronic and optical properties strongly depend on size and geometry. Surface effects also become important in thinner nanowires. GaN nanowires synthesized so far have lengths ranging from several micrometers and diameters ranging from 10 to 100 nm. GaN nanowires can provide the opportunity also to study quantum effects in one dimension theoretically, and to verify them experimentally.[8] During recent years, GaN nanowires have been synthesized by employing several different approaches, including arc discharge, laser-assisted catalytic growth, direct reaction of the mixture, hot filament chemical vapor deposition,[9] etc.

## II. HIGHLIGHTS OF THE PRESENT APPROACH

### A. Background

The growth and characteristics of GaN single crystal nanowires by our growth method, and the mechanism of their growth, were reported in the preceding papers of this series.[10–12] In this investigation our goal is to systematically study the growth method, including the effects of growth conditions ($NH_3$ flow rate, growth temperature, chamber pressure, and growth location) on the size (nano, meso, or micro) and the shape (one, two, or three dimensional), for GaN single crystal products grown by direct reaction of Ga with $NH_3$, in trying to extend the size of the nanowires from

[a)]Author to whom correspondence should be addressed; electronic mail: snmohammad2002@yahoo.com

 

the nano- to the microrange, and in modifying the dimension from one (1D; wire or rod) to two (2D; platelet, but not films), to three (3D; grain).

There are two reasons for our interest. First, as indicated earlier, free-standing materials with different sizes (e.g., nano-, meso-, and microsizes) and shapes (e.g., 1D, 2D, and 3D shapes) have various applications in electronic and optoelectronic devices.[13] For example, W wires and carbon tubes can be used as scanning tunneling microscope or atomic force microscope tips,[14] gold wires can be used as connecting wires in single electron devices, and microrods can be used as parts of nano- and microrobots.[15] There are other special properties and applications of nano- and microparticles because of their size effects.[16,17] Single crystal grains can be used as seeds for growing bulk crystals. Second, our growth method, which involves the direct reaction of Ga with $NH_3$ without use of any template[18] or catalyst,[19] is distinctly different from previous approaches. It is a vapor to solid (V-S) process.[9,10] It has the ability to grow various materials, including elements, compounds, and alloys of desired shape and size.

### B. Noteworthy features

Primary investigations reveal that a systematic and detailed study of our growth method under various conditions is very important for the following reasons. First, for GaN nanowires, the optimal growth conditions can be found for certain given shapes and sizes. These optimal conditions are indeed exciting: the growth of nanowires of uniform size and single crystal structure and of length longer than 1 mm can easily be accomplished. Second, the study provides us with significant knowledge of the details of the growth method. For example, it suggests to what degree the size, shape, composition, and structure of materials can be controlled using this growth method, and how to grow various materials. Third, because this growth method uses no template or catalyst, it has the potential to be extended to growing other kinds of materials, such as group III–V binaries (InAs and InN nanowires have already been grown in our laboratory), group II–VI binaries (ZnO), and elements (Cu,Si,Al), etc.

## III. EXPERIMENTAL METHOD

The details of the growth technique employed to synthesize the GaN nano- and microstructures can be found in Refs. 10 and 11. About 3 g of pure Ga metal was put in a BN boat (about $40\times12\times6$ $mm^3$) placed in a quartz liner (about 150 mm in length and 20 mm in outer diameter). This, in turn, was put in another larger quartz tube, called the process chamber, having 25 mm outer diameter. The liner, as shown schematically in Fig. 1, served two purposes: First, it protected the process chamber from being contaminated by products, and second, it provided the surface upon which the GaN nano- and microproducts could be formed. The process chamber was mechanically pumped down to a pressure of 30 mTorr. At the beginning of the growth process, pure $NH_3$ was passed into the system via a mass-flow controller. The process chamber was heated using a three-zone furnace for a period of 3 h during the experiment.

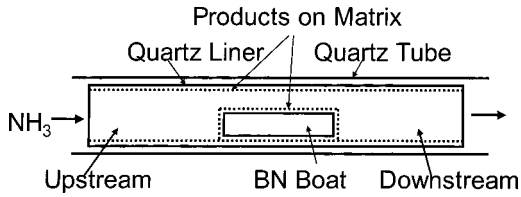


FIG. 1. Schematic diagram of the experimental setup for GaN nanowire synthesis by the direct reaction of Ga with $NH_3$.

A series of experiments were performed to change the three controllable parameters of the experiment: $NH_3$ flow rate, growth temperature, and chamber pressure. These were manipulated by changing one parameter while keeping the other two parameters constant. The $NH_3$ flow rate was varied from 20 to 150 SCCM (SCCM denotes cubic centimeters per minute at STP), the growth temperature was increased from 800 to 1100 °C, and the chamber pressure was increased from 2 to 100 Torr. GaN nano- and microproducts, formed on the BN boat and on the inner wall of the liner, are shown as the dotted line in Fig. 1. Samples were collected for measurements. The composition, structure, size, and shape of the samples were studied using optical microscopy, scanning electron microscopy (SEM), energy dispersion x-ray spectroscopy, and transmission electron microscopy.

## IV. RESULTS

### A. Local distribution of growth products along the quartz liner

Analyzing the products grown on the inside surface of the liner at 900 °C, 100 SCCM, and 15 Torr showed that there was a distribution of two distinct and easily separable products, viz., single crystal nano- and mesowires and single crystal hexagonal microplatelets. The distribution exhibited essentially the same characteristics even when the $NH_3$ flow rate differed (60–150 SCCM). Near the edge of the liner, where $NH_3$ was introduced ''upstream,'' there was a high density of wires, but no platelets at all. Moving further down the stream, it was found that the density of the wires began to diminish, and the platelets tended, in particular, to emerge as the prominent product. Figure 2(a) shows the high density of nanowires obtained near the upstream side of the liner where $NH_3$ just entered the liner. Figure 2(b) shows the partial emergence of hexagonal platelets coexisting with the nanow-

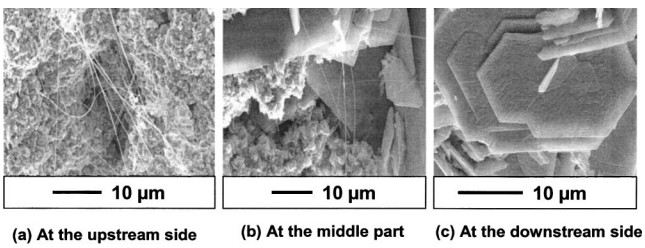


FIG. 2. SEM images of GaN samples taken from different locations of liner: (a) high density of GaN nano- and mesowires at upstream side; (b) nanowires+platelets at middle part of liner; (c) GaN hexagonal microplatelets at downstream side.

ires at the middle of the liner. At locations further down the stream, hexagonal platelets started to dominate, as shown in Fig. 2(c).

### B. Effect of chamber pressure on growth products

Varying the chamber pressure between 2 and 100 Torr, and keeping the $NH_3$ flow rate at 100 SCCM and the growth temperature at 900 °C, had a dramatic effect on the final results of the experiment. The products corresponding to 2, 5, 15, 50, and 100 Torr, respectively, and formed on the walls of the liner, could be divided into five distinct categories. At a pressure of 2 Torr, the observed GaN nanowires had high density and were observed mainly near the upstream side of the liner. The density of the nanowires decreased gradually as one moved toward the downstream side. In this area, the material was primarily polycrystalline GaN platelets formed on the wall of the liner; only polycrystalline GaN platelets were observed on the right hand end of the BN boat. At a pressure of 5 Torr, GaN nanowires formed on the walls of the liner, as well as on the BN boat, with quite high density. The nanowire density along the liner was quite uniform, and very few GaN platelets were observed on the right of the GaN boat.

The products formed on the wall of the liner at pressures of 15 and 2 Torr had some interesting features. At upstream side wires were formed at both pressures. One notable difference between the two was, however, that the GaN platelets formed at a pressure of 15 Torr were single crystals, while those formed at a pressure of 2 Torr at downstream side were polycrystalline. The distribution of products observed on the BN boat at 15 Torr was the same as that on the wall of the liner. At 50 Torr, only partial wetting of the Ga metal placed on the BN boat took place. At 100 Torr, no wetting at all was observed. Thus, no crystal products could be found either on the BN boat or on the liner wall.

### C. Effect of $NH_3$ flow rate on growth products

A series of experiments were conducted to study the effect of varying the $NH_3$ flow rate on the shape, size, and density of the nanowires. Keeping the chamber pressure constant at 15 Torr and the temperature at 900 °C, the $NH_3$ flow rate was varied between 20 and 150 SCCM. At a flow rate of 20 SCCM, only shiny Ga metal was detected [see Fig. 3(a)]. As the ammonia flow rate was increased to 30 SCCM, some polycrystalline platelets were also produced. These are shown in Fig. 3(b). As evident from Fig. 3(c), single crystal platelets with diameters of 20–40 $\mu$m began to appear at a flow rate of 30–40 SCCM. This was clear evidence of the preferential formation of big platelets at lower $NH_3$ flow rates. GaN nanowires started growing only when the flow rate reached about 40 SCCM. Figures 3(d)–3(f) show the SEM images of these nanowires grown in the flow rate range of 40 to 150 SCCM. The wires had lengths up to several hundred micrometers and diameters in the range of 80–300 nm.

As noted from Figs. 3(d)–3(f), there was no obvious increase in the product size for $NH_3$ flow rates higher than 80 SCCM. The same series of experiments were conducted by setting the temperature to 1000 and 1100 °C, respectively.

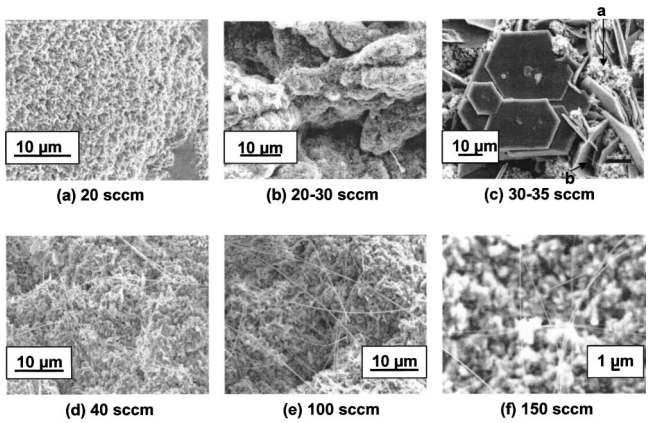


FIG. 3. SEM images of GaN products at different ammonia flow rates: (a) shiny Ga at 20 SCCM; (b) polycrystalline GaN platelets at 20–30 SCCM; (c) hexagonal GaN crystal platelets at 30–35 SCCM; (d) GaN nano- and microwires at 40 SCCM; (e) GaN nano- and microwires at 100 SCCM; (f) GaN nano- and microwires at 150 SCCM.

Essentially the same growth pattern of GaN platelets was observed for lower flow rate, with the exception that one had to decrease the flow rate much lower than 30 SCCM to obtain the GaN platelets. When we resorted to higher flow rate growth, microrods were the dominant products at a temperature of about 1000 °C, and micrograins were the dominant products at a temperature of about 1100 °C. These results will be elucidated in the growth map presented in Sec. IV E.

### D. Effect of temperature on growth products

A series of experiments were also carried out to study the effect of varying the temperature on the shapes and sizes of the GaN products. These shapes and sizes of the growth products were found to change considerably on varying the temperature between 875 and 1100 °C, but keeping the $NH_3$ flow rate constant at 100 SCCM and the chamber pressure at 15 Torr. GaN wires were grown between 825 and 875 °C with diameters of 20–130 nm, and between 875 and 950 °C with diameters of 80–300 nm. Nano- and mesowires grown at 875 and 900 °C are shown in Figs. 4(a) and 4(b), respectively. As the temperature was increased, the size increased, and microrods with diameters of 2–7 $\mu$m and lengths of 30–100 $\mu$m were produced at a temperature around 1000 °C. This is evident from Fig. 4(c). As the temperature was increased further to about 1100 °C, the growth of three-dimensional micrograins set in [see Fig. 4(d)]. The size of these micrograins was about 50–100 $\mu$m.

### E. Unified growth map

The $NH_3$ flow rate and temperature were selected as the two independent parameters for drawing the growth map. The reason for this will be discussed in Sec. V C. Growth experiments at 900, 1000, and 1100 °C, respectively, and the $NH_3$ flow rate in the range of 20–150 SCCM were carried out. With the addition of previous data[11] obtained for the temperature range of 800–875 °C, a growth map was made as shown in Fig. 5. All the samples were taken from the upstream side of the liner. When the $NH_3$ flow rate was beyond about 50 SCCM, nanowires grown from platelet

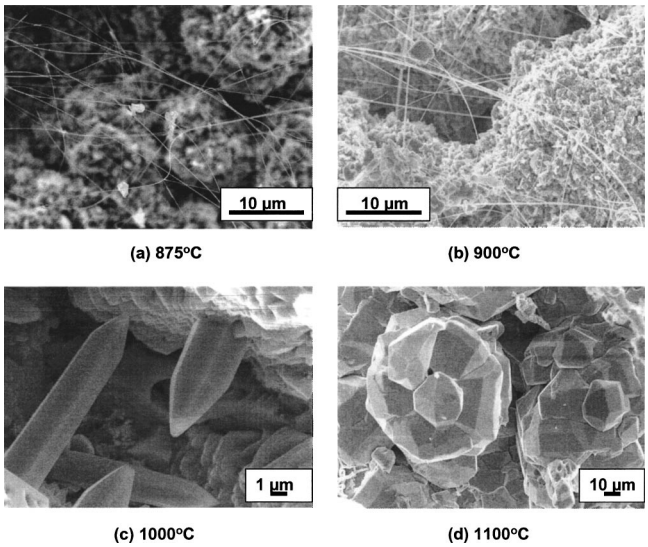


FIG. 4. SEM images of GaN products grown at different temperatures: (a) nanowires at $T=875\,^{\circ}\mathrm{C}$; (b) nano- and mesowires at $T=900\,^{\circ}\mathrm{C}$; (c) microrods at $T=1000\,^{\circ}\mathrm{C}$; (d) micrograins at $T=1100\,^{\circ}\mathrm{C}$.

edges at a temperature range of 825–875 °C, mesowires grown at temperatures between 875 and 950 °C, microrods grown at a temperature range of 950–1025 °C, and micrograins grown at a temperature range of 1025–1100 °C were obtained. With an $NH_3$ flow rate between 25 and 50 SCCM, crystalline platelets with much larger diameter and thickness were grown. For flow rates below 25 SCCM, only shiny Ga metal could be seen. Although this map presents only a rough description of the experimental results, gratifyingly, it lays down an important relationship between the experimental conditions and the shape and size of the products. In this way it gives us a clear direction for growing desired products. Notably, the growth time for all experiments was always kept at 3 h. It is likely that a different growth time would have a different growth map, which will be discussed in some detail in a subsequent report.

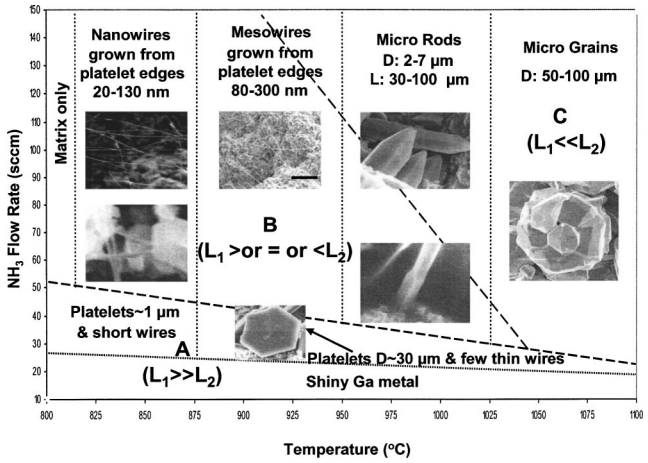


FIG. 5. Growth map showing the effects of the growth temperature and the $NH_3$ flow rate on the size and shape of products grown for 3 h.

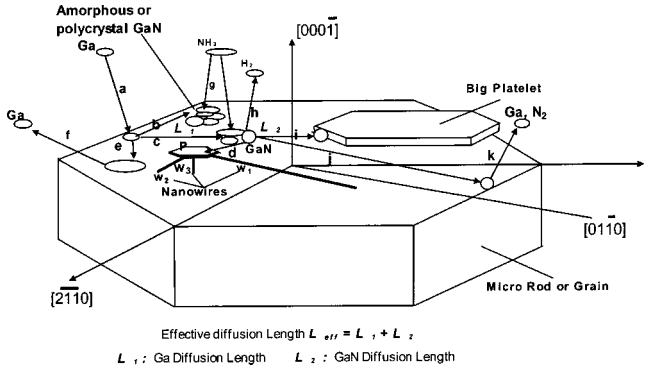


FIG. 6. An improved model for explaining the growth map.

## V. DISCUSSION

The results presented in the previous section can be better explained by introducing an effective diffusion length $L_{\mathrm{eff}}$, as shown in Fig. 6. Employing a shadowing method, Nagata and Tanaka[20] found a Ga surface diffusion length of 190 nm obtained under Ga-stable conditions. This value is much higher than 20 nm obtained by Neave *et al.*[21] under As-stable conditions. Horikoshi *et al.*[22] attributed this large difference to Ga migration on the growing surface in atomic form when in an As-free atmosphere (Ga-stable conditions) and in molecular form when in As-stable conditions. Supposedly, for growth of GaN nano- and microstructures, Ga atoms, impinging on the growth surface, migrate first in atomic form with a diffusion length $L_1$; then they meet and react with $NH_3$ producing GaN. The GaN migrates in molecular form with a diffusion length $L_2$. Thus, *an effective diffusion length* $L_{\mathrm{eff}}$ is introduced:

$$L_{\mathrm{eff}}=L_1+L_2, \tag{1}$$

where $L_1$ and $L_2$ are given by[23]

$$L_1\sim t_1^{1/2}\exp\left(-\frac{E_1}{2k_BT}\right), \tag{2}$$

$$L_2\sim t_2^{1/2}\exp\left(-\frac{E_2}{2k_BT}\right). \tag{3}$$

$t_1$ and $t_2$ are the diffusion times of Ga and GaN, respectively, on the growth surface, and $k_B$ is the Boltzmann constant. $t_1$ and $t_2$ are functions of the ratio of group-V to group-III atoms. More specifically, they are related to the ratio of the surface concentration of $NH_3$ molecules and the surface concentration of Ga atoms, viz., $n_{\mathrm{NH_3}}/n_{\mathrm{Ga}}$, which depend on $NH_3$ flow rate, Ga surface situation, pressure, geometric form of the chamber, etc. A lower V/III ratio gives a longer $t_1$ and a shorter $t_2$; a higher V/III ratio gives a shorter $t_1$ and a longer $t_2$. $E_1$ and $E_2$ are the activation energies for surface diffusion of Ga and GaN, respectively. They are related to the GaN crystal structure and the growth temperature $T$.

### A. Effect of $NH_3$ flow rate on growth products

For the sake of convenience, let us first explain the effect of the $NH_3$ flow rate on the growth products. As indicated earlier, at a temperature of 900 °C and an ammonia flow rate of 20 SCCM, only shiny Ga metal was found. In this growth

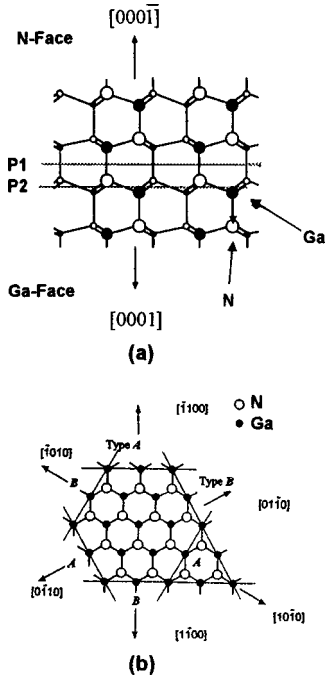


FIG. 7. (a) The cross-sectional view of hexagonally close packed wurtzite crystal structure of GaN. (b) The planview of a bilayer of hcp GaN. There are two types of growth directions expressed as A and B.

condition, the formation of GaN nanowires was very unlikely, because the amount of $NH_3$ was too little to initiate the nitridation reaction. After arriving at the growth surface Ga atoms migrated but did not undergo the nitridation reaction, following the pathway *a*-*e* shown in Fig. 6. In the above Eq. (3) $t_2=0$, $L_2=0$, and in Eq. (1) $L_{\text{eff}}=L_1$; so Ga was observed in its metallic state deposited on the walls of the quartz liner and on the BN boat. At the upstream side of the liner, small patches of polycrystals with amorphous GaN were now formed suggesting that the nitridation was very weak, as shown by the pathway *a*-*b*. As the ammonia flow rate was increased slightly, but not sufficiently to form nanowires, i.e., when $t_1 \gg t_2$, and $L_1 \gg L_2$, the Ga atoms still had a long time to migrate relatively easily. Thus, the diffusion length of Ga was still long enough to permit the growth of larger GaN platelets. This is depicted in Fig. 3(c). An important question that arises at this point is why the said growth condition allows preferentially large GaN platelets. To answer this question the dependence of $E_1$ on the crystal structure and growth direction should be taken into consideration.

Figure 7(a) shows a cross-sectional view of the hexagonally close packed (hcp) wurtzite crystal structure of a GaN crystal.[24] There are two growth faces in the basal layer: the N face $(000\bar{1})$ and the Ga face (0001). In addition, the growth rate $R[000\bar{1}]$ of the Ga face (0001) is faster[25] than that of the N face $(000\bar{1})$. Considering that N-face growth takes place first, when Ga atoms arrive at the growth surface $P1$, every Ga atom (solid circles) has only one chemical bond connecting with one N atom (open circles). But if Ga atoms arrive at the $(01\bar{1}0)$ face, which corresponds to the lateral face, based on the planview[26] of a bilayer of a hcp crystal [see Fig. 7(b)], one-half of the number of the Ga atoms, in the directions $[01\bar{1}0]$, $[1\bar{1}00]$, and $[\bar{1}010]$, have two bonds connecting with two N atoms; the other half of the Ga atoms, in the directions $[0\bar{1}10]$, $[\bar{1}100]$, and $[10\bar{1}0]$, have one bond connecting with one N atom. Therefore, on average, every Ga atom has one and one-half bonds connecting with N atoms. This means that $E_1(000\bar{1})$ should be less than $E_1(01\bar{1}0)$ and all other $E_1$ values of the lateral face. According to Eq. (2), this would result in *anisotropy of* $L_1$ *and the growth rate* $R$: $L_1(000\bar{1})$ on the $(000\bar{1})$ face would be longer than $L_1(01\bar{1}0)$ on the $(01\bar{1}0)$ face; and the growth rate $R[000\bar{1}]$ in the $[000\bar{1}]$ direction would be slower than the growth rate $R[01\bar{1}0]$ in the $[01\bar{1}0]$ direction. Consequently, the basal face $(000\bar{1})$ of the platelets would be larger than the lateral face $(01\bar{1}0)$ of the platelets, as shown in Fig. 3(c). The diameter of the large platelets shown in this figure is 20–40 $\mu$m and the thickness is $\sim$1 $\mu$m. In model Fig. 6, the pathway a-c-i finally gives rise to large platelets. When the ammonia flow rate is decreased further to 20–30 SCCM, a polycrystal was formed, but still rough large platelets appeared, as shown in Fig. 3(b). As to the Ga face (0001) growth, when Ga atoms arrive at growth face $P2$, every Ga atom has three bonds connecting with three N atoms, as shown in Fig. 7(a). Therefore, $E_1(0001) \gg E_1(000\bar{1})$ and also $E_1(000\bar{1}) > E_1(01\bar{1}0)$, resulting in $L_1(0001) \ll L_1(000\bar{1})$ and $L_1(000\bar{1}) < L_1(01\bar{1}0)$ and growth rates $R[0001] \gg R[000\bar{1}]$ and $R[000\bar{1}] > R[01\bar{1}0]$. But, unfortunately, the higher growth rate $R[0001]$ of Ga-face growth could not be realized because of very low ammonia flow rate. There are two possibilities where products could form: amorphous GaN mixed with polycrystalline GaN indicated by arrow **a** as shown in Fig. 3(c); and a few thin wires with possible [0001] growth direction indicated by arrow **b**, as shown at the lower right corner in Fig. 3(c).

No significant changes in the size of the GaN nanowires were observed as the ammonia flow rate was increased higher than 40 SCCM up to a value of 150 SCCM. However, there was a considerable increase in the density of the wires along the quartz liner. One can see from Eqs. (2) and (3) that, as the $NH_3$ flow rate was increased, the V/III ratio also increased. This led to $t_2 \approx t_1$, implying that $t_2$ was longer than or equal to or shorter than $t_1$, but the two were not very different. The diameter of the platelets was about 1 $\mu$m, the thickness was 20 nm to several hundreds of nanometers, and the ratio of the diameter to the thickness was about 3:1. Both diameter and thickness were much smaller than those of platelets grown with a $NH_3$ flow rate lower than 40 SCCM. Considering the anisotropy of $L_1$ during $t_1$, this result is reasonable. Limited by $L_{\text{eff}}$, the platelet $P$ in the model could not continue growth for an infinite period of time in single crystal form. The pathway was *a*-*c*-*d*. Nanowires $W_1$ in the growth direction $[01\bar{1}0]$ and nanowires $W_2$ in the growth direction $[2\bar{1}10]$ grew from the edges of the platelets $P$ as shown in the growth map Fig. 5 at temperature from 825 to 875 °C, and will be discussed in Sec. V D. The diameter of the nanowires depended on the thickness of the platelets. The thickness of the platelets also depended on $L_{\text{eff}}$ of the $(01\bar{1}0)$ or $(0\bar{1}10)$ face. Both the diameter of the wires and the thick-

ness of the platelets were, therefore, functions of the growth temperature $T$ and the ratio $n_{NH_3}/n_{Ga}$ (the flow rate in this experiment). Nanowires $W_3$ in the growth direction [0001] grew from the (0001) face because of the higher growth rate and shorter diffusion length in the [0001] direction as discussed above. Further increase of the $NH_3$ flow rate led only to an increase in the density of the nanowires.

The same results, but with different products (microrods and micrograins) were obtained at higher temperatures with the exception that one had to decrease the flow rate much lower than 30 SCCM to obtain the GaN platelets. This is because, as the temperature was increased, the ammonia dissociation became easier and faster.[26,27] Also there was no significant change in the size as the ammonia flow rate was increased for most wires.

### B. Local distribution of growth products along the quartz liner

The results presented in Sec. IV B provoked the question of whether nanowires and hexagonal microplatelets are related to the location at a pressure of 15 Torr. In the reaction area on or above the surface of the matrix, the concentration of Ga atoms was uniform in the entire liner; but after the reaction

$$2Ga + 2NH_3 \rightarrow 2GaN + 3H_2, \tag{4}$$

$NH_3$ in the central axial area of the liner diffused onto the liner wall to continue nitridation. The $H_2$ thus released from the reaction (4) diffused into the volume of the liner. It was then exhausted out. However, if some experimental condition (for example, higher pressure) could cause the diffusion speed to be too low, at locations toward the downstream side, the $NH_3$ concentration on or above the surface of the matrix would decrease, and in contrast the $H_2$ concentration would increase. On the downstream side the decrease of the $NH_3$ concentration decreased the $NH_3$ arrival rate; and the increase of the $H_2$ concentration decreased the speed of reaction (4). An inspection of Eq. (3) suggests that a lower $NH_3$ arrival rate (lower ratio $n_{NH_3}/n_{Ga}$) gives a longer $t_1$ and shorter $t_2$, which causes the Ga diffusion length to be longer at the upstream than at the downstream side. For the same reason (as described in Sec. V A), GaN hexagonal microplatelets were formed at the downstream side of the liner, while GaN nanowires grew at the upstream side. Note that (a) for this reason the higher the growth temperature, the more obvious this uniformity of the distribution; (b) variation of the growth chamber geometric parameters also influences the local distribution of growth products, so in this experiment all chamber geometric parameters were the same; (c) the uniformity of the distribution could be improved by changing the chamber pressure; the fundamental cause for this is explained in Sec. V C.

### C. Effect of chamber pressure on growth products

The best results obtained from our experiments were those for the chamber pressure 5 Torr at 875 °C and 100 SCCM. This can be explained by noting that, at this pressure, the $NH_3$ flow was laminar and the velocity of $NH_3$ molecules was optimal, which gave rise to a uniform distribution of $NH_3$ molecules along the liner. At a lower chamber pressure of 2 Torr the flow of $NH_3$ was turbulent, and the high velocity of $NH_3$ molecules resulted in scattering off the linear wall and the boat, thus reducing the chances of adsorption of $NH_3$ molecules on the surface of Ga. Based on Eq. (3), if the $NH_3$ arrival rate was low (i.e., a lower ratio $n_{NH_3}/n_{Ga}$), Ga atoms would have a longer diffusion length. For the same reason, as we saw in Sec. IV A, a larger $L_1$ resulted in the formation of hexagonal platelets. At a higher chamber pressure of 15 Torr, the velocity of $NH_3$ molecules was very low. So, following the reaction Eq. (4), $H_2$ molecules could not be pumped out rapidly. Thus $H_2$ accumulated on the Ga surface, thus hindering $NH_3$ arrival. Therefore, some platelets were formed, especially downstream. As the pressure became higher than 50 Torr, the Ga metal could no longer be wetted. It is noteworthy that the optimum pressure is different in different experimental conditions; therefore, the optimum pressure should be determined by experiment.

Summarizing the results of Secs. IV A to IV C, it is quite evident that growth parameters such as $NH_3$ flow rate, growth location, and chamber pressure all have a profound effect on the size, shape, and density of the products. However, the primary influence comes from the $NH_3$ arrival rate and the consequent $NH_3$ surface concentration $n_{NH_3}$. This implies that we can express the effects of the above growth parameters, i.e., $NH_3$ flow rate, location and geometric parameters of the growth chamber, and chamber pressure, on product morphology in terms of the $NH_3$ arrival rate, which dictates the ratio $n_{NH_3}/n_{Ga}$. If the location of taking samples, the geometric parameters of the growth chamber, and the chamber pressure are kept fixed, and the density of the Ga vapor depends only on temperature and location, then the $NH_3$ flow rate acts as the sole parameter controlling $n_{NH_3}$. In this way, the ammonia flow rate and temperature determine the effects on the shape and size of the products. This is the reason why, in Sec. IV E, the $NH_3$ flow rate and temperature alone appeared to be sufficient as the two independent parameters to allow the drawing of the growth map.

### D. Growth map and effect of temperature on growth products

For the sake of convenience, the growth map and the effect of temperature on the growth products are discussed together. In accordance with the observed results and our growth model, the growth map can be divided into three zones by drawing two dashed lines, as shown in Fig. 5. In zone A the flow rate was lower than 50 SCCM. From Eqs. (2) and (3) we note that $L_1 \gg L_2 \rightarrow 0$. Ga atomic surface diffusion played the main role. Between 25 and 50 SCCM, because $E_1(0001) < E_1(0110)$, we have $L_1(0001) \gg L_1(0110)$ and the growth rate $R[0001] \ll R[0110]$. After arrival at the growth surface Ga atoms migrated a very long distance $L_1$, then reacted with $NH_3$, and finally migrated a very short distance $L_2$ to form large, but thin, platelets. These are shown in the model of Fig. 6 as pathway $a-c-i-$big platelets. The diameter of the platelets increased as the temperature was raised. The dashed line goes down at higher

temperature $T$, because there is a higher dissociation rate of $NH_3$ at higher temperature. When the flow rate was lower than about 25 SCCM, the product was nearly all shiny Ga metal along the pathway $a$-$e$ or a GaN polycrystal $a$-$b$. In zone B the flow rate is higher than that in zone A, resulting in $L_1 \sim L_2$. So the Ga diffusion length and the GaN diffusion length play the same role. However, during the Ga diffusion period, the condition $E_1(0001) < E_1(01\bar{1}0)$ still favored platelet growth. With the temperature between 800 and 820 °C, both $L_1$ and $L_2$ were very short, and GaN was formed only as small polycrystals mixed together with an amorphous matrix along the pathway $a$-$b$ of Fig. 6. As the temperature $T$ was increased from 820 to 950 °C, $L_1$ decreased, and the condition $L_1 > L_2$ changed to the new condition $L_1 = L_2$ or $L_1 < L_2$. So $E_1(0001) < E_1(01\bar{1}0)$ still favored platelet growth during the Ga diffusion period. After nitridation, the GaN molecule diffused along the pathway $a$-$c$-$d$ and formed platelets $P$ with diameter of $\sim$1–2 $\mu$m and thickness ranging from 20 nm to several hundreds of nanometers. The platelet $P$ could not continue growing as a single crystal for an indefinite period of time because of the limit on $L_{\text{eff}}$. If the platelets $P$ continue growing, their crystal structure may not be single crystal. Once a single crystal nanowire formed, its structure is stable because the energy state of a single crystal nanowire structure is lower than those of polycrystal or amorphous structures. So nanowires $W_1$ along the direction $[01\bar{1}0]$ or nanowires $W_2$ along the direction $[2\bar{1}10]$ grew from the platelet edges, as shown in Fig. 6 (pathway $a$-$c$-$d$-$P$-$W_1$ or $W_2$). The diameter of these nanowires depended on the thickness of the platelets, and hence it increased with increasing temperature $T$. For temperatures between 950 and 1000 °C, the tendency of growth was the same as below 950 °C, except that, for the latter, the flow rate should be lower than about 80 SCCM, allowing microrods to be formed from the thick platelet edges. The highest flow rate was for zone C, which corresponds to temperatures higher than 1000 °C and flow rates higher than $\sim$30 SCCM. At temperatures higher than 1000 °C, the dissociation rate of $NH_3$ was very fast and the Ga vapor pressure was high. Once Ga atoms arrived on the growth surface, GaN was formed. This caused $t_1 \rightarrow 0$ and $0 \leftarrow L_1 \ll L_2$; so $L_{\text{eff}} = L_2$. To our knowledge the physical picture of GaN molecular surface diffusion is not clear. Suppose that there is isotropy in $E_2$, viz., $E_2(0001) = E_2(01\bar{1}0)$. So $L_2(0001) = L_2(01\bar{1}0)$ and the growth rate $R[0001] = R[01\bar{1}0]$. For temperatures between 950 and 1000 °C and flow rates higher than 80 SCCM, the size of the lateral face in the $[01\bar{1}0]$ direction reached its maximum length $L_2$ causing single crystal growth to stop. However, the basal face in the direction [0001] still allowed growth without interruption. In this case, microrods were grown in the growth direction $[000\bar{1}]$ or [0001]. When the temperature rose to 1100 °C, since a growth time of three hours did not appear to be long enough for the growth in the $[01\bar{1}0]$ direction to reach its maximum length $L_2$ and the growth rates in all directions were the same, micrograin growth resulted. The pathway for zone C is $a$-$c$-$j$ in Fig. 6.

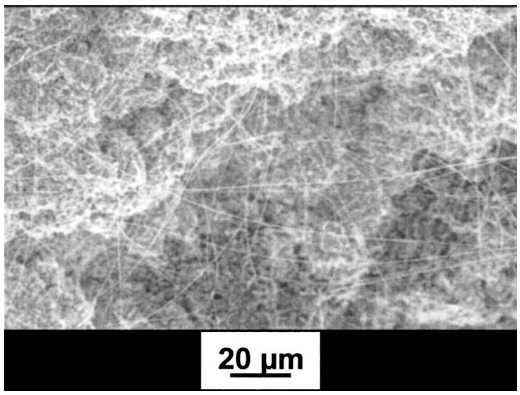


FIG. 8. A typical SEM image of nanowires synthesized under optimal growth conditions. For this, the growth temperature was 875 °C, the $NH_3$ flow rate was 100 SCCM, the chamber pressure was 5 Torr, the Ga amount was 6 g, and the growth duration was 6 h.

## VI. CONCLUSION

A series of experiments have been performed for a systematic study of the effects of growth parameters on the shape and size of crystal products. A growth map with a wider range of experimental parameters can thus be proposed. The map has three distinct zones. The shape and the size of the products in every zone depend on the growth temperature and the $NH_3$ flow rate. If an effective surface diffusion length, which comprises the anisotropy of the Ga surface diffusion length, and the anisotropy of the growth rate are introduced into the growth model, it is striking that all the observed results can be successfully explained. This is indeed a very important observation. The optimal growth parameters were determined for 875 °C and 100 SCCM. One remarkable observation is the formation of nanowires with uniform diameter, clear crystal structure, and length larger than 1 mm; the location distribution is also uniform and the yield is quite high. All these results are evident from Fig. 8. The growth map gives a clear direction of how to successfully obtain nano-, meso-, and microproducts in 1D, 2D, and 3D. It is indeed exciting.

## ACKNOWLEDGMENTS

This research was supported by the Air Force Office of Scientific Research, Grant No. F49620-02-1-0008 monitored by Major Daniel K. Johnstone Ph.D. and Lt.Col. Todd Steiner Ph.D. The authors gratefully acknowledge Professor J. B. Halpern for helpful discussions, and J. Griffin, C. Taylor, and T. Gomez for technical help.

[1] Z. H. Wu, X. Y. Mei, D. Kim, M. Blumin, and H. E. Ruda, Appl. Phys. Lett. **81**, 5177 (2002).
[2] A. D. Berry, R. J. Tonucci, and M. Fatemi, Appl. Phys. Lett. **69**, 2846 (1996).
[3] Hanxuan Li, Theda Daniels-Race, and Mohamed-Ali Hasan, J. Vac. Sci. Technol. B **19**, 1471 (2001).
[4] Haeyeon Yang, P. Ballet, and G. J. Salamo, J. Appl. Phys. **89**, 7871 (2001).
[5] N. Kouklin, L. Menon, A. Z. Wong, D. W. Thompson, J. A. Woollam, P. F. Williams, and S. Bandyopadhyay, Appl. Phys. Lett. **79**, 4423 (2001).
[6] S. N. Mohammad and H. Morkoç, Prog. Quantum Electron. **20**, 361 (1996).
[7] H. Morkoç and S. N. Mohammad, Science **267**, 51 (1995); G. Fasol, *ibid.* **272**, 1751 (1996); F. A. Ponce and D. P. Bour, Nature (London) **368**, 351

(1997); J. R. Kim, H. M. So, J. W. Park, J. J. Kim, J. Kim, C. J. Lee, and S. C. Lyu, Appl. Phys. Lett. **80**, 3548 (2002); M. W. Lee, H. Z. Twu, C. C. Chen, and C. H. Chen, *ibid.* **79**, 3693 (2001); G. L. Harris, P. Zhou, M. Maoqi, and J. B. Halpern, in *Technical Digest, Lasers and Electro-Optics, 2001: CLEO '01*, 239.

[8] S. M. Lee, Y. H. Lee, Y. G. Hwang, J. Elsner, and D. Porezag, Phys. Rev. B **60**, 7788 (1999).

[9] W. Han, S. Fan, Q. Li, and Y. Hu, Science **277**, 1287 (1997); X. F. Duan and C. M. Lieber, J. Am. Chem. Soc. **122**, 188 (2000); C. C. Chen and C. C. Yeh, Adv. Mater. (Weinheim, Ger.) **12**, 738 (2000); X. Chen, J. Li, Y. Cao, Y. Lan, H. Li, M. He, C. Wand, Z. Zhang, and Z. Qiao, *ibid.* **12**, 1437 (2000); G. S. Cheng, L. D. Zhang, Y. Zhu, G. T. Fei, and L. Li, Appl. Phys. Lett. **75**, 2455 (1999); C. C. Tang, S. Fan, H. Y. Dand, P. Li, and Y. M. Liu, *ibid.* **77**, 1961 (2000); H. Y. Peng, X. T. Zhou, N. Wang, Y. F. Zheng, L. S. Liao, W. S. Shi, G. S. Lee, and S. T. Lee, Chem. Phys. Lett. **327**, 263 (2000); Wei-Qiang Han and A. Zettl, Appl. Phys. Lett. **81**, 5051 (2002).

[10] Maoqi He, I. Minus, P. Zhou, S. N. Mohammad, J. B. Halpern, R. Jacobs, W. L. Sarney, L. Salamanca-Riba, and R. D. Vispute, Appl. Phys. Lett. **77**, 3731 (2000).

[11] Maoqi He, P. Zhou, S. N. Mohammad, G. L. Harris, J. B. Halpern, R. Jacobs, W. L. Sarrey, and L. Salamanca-Riba, J. Cryst. Growth **231**, 357 (2001).

[12] R. Jacobs, L. Salamanca-Riba, Maoqi He, G. L. Harris, P. Zhou, S. N. Mohammad, and J. B. Halpern, Mater. Res. Soc. Symp. Proc. **675**, W9.4.1 (2001).

[13] X. Duan, Y. Huang, R. Agarwal, and C. M. Lieber, Nature (London) **421**, 241 (2003).

[14] E. S. Snow, P. M. Campbell, and J. P. Novak, J. Vac. Sci. Technol. B **20**, 822 (2002).

[15] N. C. MacDonald, in *Nanotechnology*, edited by G. Timp (Springer-Verlag, New York, 1999), Chap. 3.

[16] S. Pilgram and M. Buttiker, Phys. Rev. Lett. **89**, 200401 (2002).

[17] W. Han, S. Fan, Q. Li, and Y. Hu, Science **277**, 1287 (1997).

[18] Y. M. Wang, M. W. Chen, F. H. Zhou, and E. Ma, Nature (London) **419**, 912 (2002).

[19] C. C. Chen and C. C. Yen, Adv. Mater. (Weinheim, Ger.) **12**, 738 (2000).

[20] S. Nagata and T. Tanaka, J. Appl. Phys. **48**, 940 (1977).

[21] J. H. Neave, P. J. Dobson, B. A. Joyce, and J. Zhang, Appl. Phys. Lett. **47**, 100 (1985).

[22] Y. Horikoshi, M. Kawashima, and H. Yamaguchi, Jpn. J. Appl. Phys., Part 2 **25**, L868 (1986).

[23] *Thin-Film Deposition: Principles and Practice*, edited by Donald L. Smith (McGraw-Hill, New York, 1995), p. 135.

[24] J. L. Rouviere, J. L. Weyher, M. Seelmann-Eggebert, and S. Porowski, Appl. Phys. Lett. **73**, 668 (1998).

[25] J. L. Rouviere, M. Arlery, R. Niebuhr, K. H. Bachem, and O. Briot, Mater. Sci. Eng., B **43**, 161 (1997).

[26] M. H. Xie, S. M. Seutter, W. K. Zhu, L. X. Zheng, H. S. Wu, and S. Y. Tong, Phys. Rev. Lett. **82**, 2749 (1999).

[27] M. Kamp, M. Mayer, A. Pelzmann, and K. J. Ebiling, MRS Internet J. Nitride Semicond. Res. **2**, 26 (1997).